

# Exploration of a Slotted Laminar-Flow-Control Airfoil Concept

## Final Technical Report - NASA Grant No. NNX13AB86A

Mark D. Maughmer and Amandeep Premi  
Department of Aerospace Engineering  
Penn State University

Dan M. Somers  
Airfoils, Incorporated

### Abstract

The S414, slotted, natural-laminar-flow (SNLF) airfoil was investigated in the Pennsylvania State University Low-Speed, Low-Turbulence Wind Tunnel to explore practical aspects of the two-element, SNLF concept. The extensive testing increased the understanding of the aerodynamic interaction between the fore and aft elements. The results confirm the potential of the SNLF concept and provide a better understanding of the use of the aft element as a control surface. The section characteristics of the S414 airfoil are compared with those of a laminar-flow-control airfoil, the DLR LAMA1, which employs boundary-layer suction. Comparisons of the theoretical and experimental results for both airfoils show good agreement.

### Nomenclature

$c$	=	airfoil chord
$c_d$	=	profile-drag coefficient
$c_l$	=	section lift coefficient
$c_m$	=	section pitching-moment coefficient about quarter-chord point
$p$	=	static pressure
$q$	=	dynamic pressure
$x$	=	airfoil abscissa
$C_p$	=	pressure coefficient, $(p_l - p_\infty)/q_\infty$
$L.$	=	lower surface
$R$	=	Reynolds number based on free-stream conditions and airfoil chord
$S.$	=	boundary-layer separation location, $x_s/c$
$T.$	=	boundary-layer transition location, $x_T/c$
$U.$	=	upper surface
$\alpha$	=	angle of attack relative to x-axis, deg
$\delta_f$	=	aft-element incidence, deg

### Subscripts

$l$	local point on airfoil
max	maximum
$S$	separation
$T$	transition
$\infty$	free-stream conditions

## Introduction

Owing to the recent increase in fuel prices, interest in laminar-flow technologies has surged. Active laminar-flow-control technologies, such as those using suction to increase the extent of laminar flow, are being revisited in search of practical solutions. These active techniques suffer, however, from practical drawbacks due to the complexity of the required systems and consequent additional weight and cost. The technique of passively shaping a single-element airfoil to increase the extent of natural laminar flow (NLF) does not share these disadvantages, but it is limited by the trade-off between the extent of laminar flow and the achievable maximum lift coefficient.

The two-element, slotted, natural-laminar-flow (SNLF) airfoil concept is a passive, NLF concept aimed at achieving a high maximum lift coefficient and extensive laminar flow in cruise [1]. The aft element allows favorable pressure gradients over the entire fore element, which results in 100-percent-chord laminar flow on that element, while the aft element achieves laminar flow over roughly 60 percent of the upper surface and 100 percent of the lower. The overall result is an airfoil that achieves laminar flow over all but about 10 percent of the entire surface. The potential of the SNLF concept has been previously demonstrated through wind-tunnel investigations of the S103 airfoil in the NASA Langley Low-Turbulence Pressure Tunnel (LTPT) [2], and the S414 airfoil in the Penn State Low-Speed, Low-Turbulence Wind Tunnel (LSLTT) [3].

The overall aim of the effort reported herein is to improve on the earlier SNLF designs to advance the SNLF concept toward practical application. To accomplish this goal, a better understanding of the aerodynamics is sought through experimental exploration of different configurations of the fore and aft elements of the S414 airfoil. The effort also includes theoretical tool development for laminar-flow-control (LFC) airfoil design using suction. The results obtained provide crucial understanding for the design of more practical SNLF and LFC airfoils. They also help facilitate meaningful comparisons of practical applications of these different laminar-flow technologies to conceptual vehicle design. The research conducted included a wind-tunnel investigation of the S414 airfoil, shown in Fig. 1, and analysis of the wind-tunnel data for a suction LFC airfoil, the LAMA1. This airfoil, shown in Fig. 2, was designed by the first author and tested earlier at the Deutsche Forschungsanstalt für Luft- und Raumfahrt (DLR, the German Research Institute for Aviation and Space Flight) in Braunschweig.

## Objectives

The primary objective of the S414 wind-tunnel investigation is to achieve a better understanding of the aerodynamics and practicality of the SNLF airfoil concept. The experimental results benefit feasibility assessments of the SNLF concept, as well as validate the SNLF airfoil design tools. Likewise, the increased understanding provides critical guidance for the design of SNLF airfoils having more docile stall characteristics and even lower profile drag.

Similar benefits result from revisiting the design process and wind-tunnel measurements of the DLR LAMA1 LFC airfoil. The high-quality, DLR wind-tunnel results have never been compared with theoretical predictions, or used to validate the

airfoil design process. Given the current interest in LFC, along with the scarcity of suitable data, the benefits of exploring these results are numerous. Finally, the outcome of these complimentary activities facilitates a cursory but meaningful comparison of the SNLF and LFC concepts.

## **Experimental Procedure**

### **Wind Tunnel**

The Pennsylvania State University Low-Speed, Low-Turbulence Wind Tunnel, shown in Fig. 3, is a closed-throat, single-return, atmospheric tunnel [4]. The test section is 101.3 cm (39.9 in.) high by 147.6 cm (58.1 in.) wide. The corners of the test section are filleted. Airfoil models are mounted vertically and attached to computer-controlled turntables that allow the model angle of attack to be set. The turntables are flush with the floor and ceiling and rotate with the model. The axis of rotation is typically the model midchord. The gaps between the model and the turntables are sealed. At a velocity of 46 m/s (150 ft/s), the flow angularity is everywhere below  $\pm 0.25$  degrees in the test section. At this velocity, the mean velocity variation in the test section is below  $\pm 0.2$  percent, and the turbulence intensity is less than 0.045 percent. The flow quality is well-documented, and the facility qualified by comparing airfoil measurements performed in it with those obtained in other highly-regarded low-turbulence wind-tunnel facilities [4].

### **Model**

The aluminum model of the S414 airfoil was fabricated by Advanced Technologies, Incorporated, Newport News, Virginia, using a numerically-controlled milling machine. The model has a chord of 457.2 mm (18.00 in.) and a span of 107.95 cm (42.50 in.) and, thus, extended through both turntables. Upper- and lower-surface, static-pressure orifices are located to one side of midspan and are staggered spanwise to minimize the influence of the orifices on boundary-layer transition. All the orifices are 0.51 mm (0.020 in) in diameter with their axes perpendicular to the surface. The surface of the model was sanded to ensure an aerodynamically smooth finish. The measured model contour is within 0.13 mm (0.005 in) of the prescribed shape.

### **Tests**

To better understand the various aerodynamic phenomena involved in the SNLF airfoil concept and to explore the use of the aft element as a control surface, a number of configurations of the two elements of the S414 airfoil, as indicated in Table 1, were investigated. In addition, a simple flap was incorporated into the aft element. Finally, the drag of aft-element mounting brackets was measured. All the tests were performed at a Reynolds number of  $1.0 \times 10^6$  and a Mach number of 0.1 with transition free. The effect of fixing transition on both the fore and aft elements was determined previously [3]. As presented in Fig. 4, the comparison between the section characteristics of the current

baseline configuration and those of the same configuration measured in 2009 is excellent [3]. This level of repeatability is typical of the facility.

## **Discussion of Results**

### **Effect of Aft-Element Incidence**

Pressure distributions for a range of angles of attack for the baseline configuration are shown in Fig. 5. The pressure distribution on the aft element changes little with angle of attack. Altering the incidence of the aft element, however, has a large effect on the pressure distributions on both the aft and fore elements. The effect is illustrated by comparing the pressure distribution for the baseline configuration, shown at a lift coefficient of approximately 0.5 in Fig. 6, to the pressure distributions with aft-element incidences of -5 and 5 degrees at about the same lift coefficient, as shown in Figs. 7 and 8, respectively. Decreasing the incidence reduces the circulation on the aft element, which eliminates the favorable pressure gradient along the cove region of the fore-element lower surface, as shown in Fig. 7. Increasing the incidence increases the circulation on the aft element, which leads to pressure peaks on the aft element and in the cove region of the fore element, as shown in Fig. 8.

The effect of the increased aft-element incidence on the section characteristics is shown in Fig. 9. Although the profile-drag coefficients more than double, the maximum lift coefficient is essentially unaffected.

### **Effect of Aft-Element Translation**

Translating the aft element forward and aft has effects on the pressure distributions, Figs. 10 and 11, respectively, that are similar to those resulting from increasing and decreasing the incidence of the aft element. The effect on the section characteristics of an aft translation of the aft element relative to those of the baseline configuration are presented in Fig. 12.

### **Effect of Aft-Element Rotation Plus Translation**

Although the section characteristics of the aft-element positions discussed thus far, Figs. 9 and 12, show little effect on the maximum lift coefficient and significant increases in the profile-drag coefficient, combining an aft-element rotation and translation can lead to an increase in maximum lift coefficient and an upward shift of the low-drag, lift-coefficient range, as shown in Fig. 13.

### **Effect of Aft-Element Simple Flap**

The results for a combined aft-element rotation and translation suggest that a schedule of aft-element positions could be developed for roll control and/or high lift, but a simple flap incorporated into the aft element may be more practical. Such a simple flap was simulated by adding a tab to the trailing edge of the aft element, as shown in Fig. 14.

The effect of deflecting the simple flap on the section characteristics is summarized in Fig. 15. By producing significant changes in lift without unacceptable increases in drag, the simple flap appears to be suitable for control and high-lift purposes.

Finally, the parasitic drag from the mounting brackets used to attach the aft element to the fore element was also measured and found to be acceptable.

### **Comparison of Theoretical and Experimental Results**

Oil-flow visualization was used to validate the transition locations predicted by the method of Ref. [6]. The photograph shown in Fig. 16 confirms the achievement of full-chord laminar flow on the upper surface of the fore element and over more than 60 percent of the upper surface of the aft element.

The comparison of the section characteristics predicted using the methods of Refs. [6, 7] with the wind-tunnel measurements is shown in Fig. 17. The agreement between the predicted and measured drag polars is remarkably good, and although both theoretical methods overpredict the maximum lift coefficient and the magnitude of the pitching-moment coefficient, the overall agreement is regarded as good, especially considering the complexity of the two-element configuration.

The section characteristics predicted for the DLR LAMA1 suction airfoil using the methods of Refs. [8-10] are compared with the measurements made in the DLR wind-tunnel in Fig. 18. The agreement is also considered to be remarkably good, especially given the complexity of the suction airfoil.

### **Comparison of SNLF and LFC Airfoils**

A comparison of the experimental section characteristics of the S414 SNLF airfoil and the DLR LAMA1 LFC airfoil is shown in Fig. 19. It should be noted that the S414 airfoil is intended for use on a helicopter rotor, whereas the LAMA1 airfoil is intended for use on a sailplane and, thus, the comparison is not strict. In addition, the measurements were made in two different wind tunnels and, while ideal suction requirements are included, the profile-drag coefficients of the LAMA1 LFC airfoil do not include any losses in the suction system. The LFC airfoil exhibits lower profile-drag coefficients, whereas the SNLF airfoil achieves a higher maximum lift coefficient. Both advantages lead to lower wing profile drag.

### **Concluding Remarks**

The S414, slotted, natural-laminar-flow (SNLF) airfoil was investigated in the Pennsylvania State University Low-Speed, Low-Turbulence Wind Tunnel to explore practical aspects of the two-element, SNLF concept. The extensive testing increased the understanding of the aerodynamic interaction between the fore and aft elements. The results confirm the potential of the SNLF concept and provide a better understanding of the use of the aft element as a control surface. While an aft-element position schedule is feasible for roll control and/or high lift, the incorporation of a simple flap into the aft element appears to be a more practical solution. The abrupt stall characteristics of the

S414 SNLF airfoil are unacceptable and their mitigation is a major design goal for future SNLF airfoils.

The section characteristics of the SNLF airfoil have been compared with those of a laminar-flow-control (LFC) airfoil, the DLR LAMA1, which employs suction. The comparison illustrates the interesting possibilities presented by the two concepts. The LFC airfoil exhibits lower profile-drag coefficients, whereas the SNLF airfoil achieves a higher maximum lift coefficient. As the higher maximum lift of the SNLF concept can result in less wing area for a given stall speed, both approaches can lead to overall lower wing profile drag,

The comparisons between the theoretical and experimental results for both airfoils show good agreement, except for the maximum lift coefficient and the stall characteristics. Such discrepancies are typical even of predictions for fixed-geometry, single-element airfoils.

The improved aerodynamic understanding and the theoretical tool validation will allow for the design of more realistic and practical airfoils employing both laminar-flow technologies. This will permit more meaningful trade studies for aircraft employing these approaches, and ultimately, more advanced SNLF and LFC airfoils should result in the practical application of these technologies.

### **Acknowledgements**

The effort was sponsored by the National Aeronautics and Space Administration under award no. NNX13AB86A. James M. Luckring served as the technical monitor. Any opinions, findings, and conclusions or recommendations expressed in this material are those of the authors and do not necessarily reflect the views of the National Aeronautics and Space Administration.

### **References**

- [1] Somers, Dan M., "Laminar-Flow Airfoil," U.S. Patent 6,905,092 B2, June 2005.
- [2] Somers, Dan M., "An Exploratory Investigation of a Slotted, Natural-Laminar-Flow Airfoil," NASA CR-2012-217560, 2012.
- [3] Somers, Dan M. and Maughmer, Mark D., "Design and Experimental Results for the S414 Airfoil," U.S. Army Research, Development and Engineering Command, RDECOM TR 10-D-112, Aug. 2010.
- [4] Premi, A. and Maughmer, M.D., "Flow-Quality Measurements and Qualification of the Pennsylvania State University Low-Speed, Low-Turbulence Wind Tunnel," 50<sup>th</sup> AIAA Aerospace Sciences Meeting, Jan. 2012.
- [5] Somers, Dan M., "Design and Experimental Results for the S805 Airfoil," National Renewable Energy Laboratory, NREL/SR-440-6917, Jan. 1997.

- [6] Drela, M., "Design and Optimization Method for Multi-Element Airfoils," AIAA Paper 93-0969, Feb. 1993.
- [7] Nichols, R. and Buning, P. G., "User's Manual for OVERFLOW 2.1, Version 2.1t," NASA Langley Research Center, Hampton, VA, Aug. 2008.
- [8] Eppler, Richard, "Airfoil Program System 'PROFIL07'. User's Guide," Richard Eppler, c.2007.
- [9] Drela, M. and Youngren, H., "XFOIL 6.94 User Guide," Massachusetts Institute Technology, Cambridge, MA, 1996.
- [10] ANSYS® Fluent 12.0 User Guide, ANSYS, Inc.

Position	$\delta$ (aft-element incidence)							F (simple flap)		
1	0	1	5	10	-5	-10	-15			
1+F	0							3.5	22.5	-17
2	0	5	10							
3	2	5								
4	0									

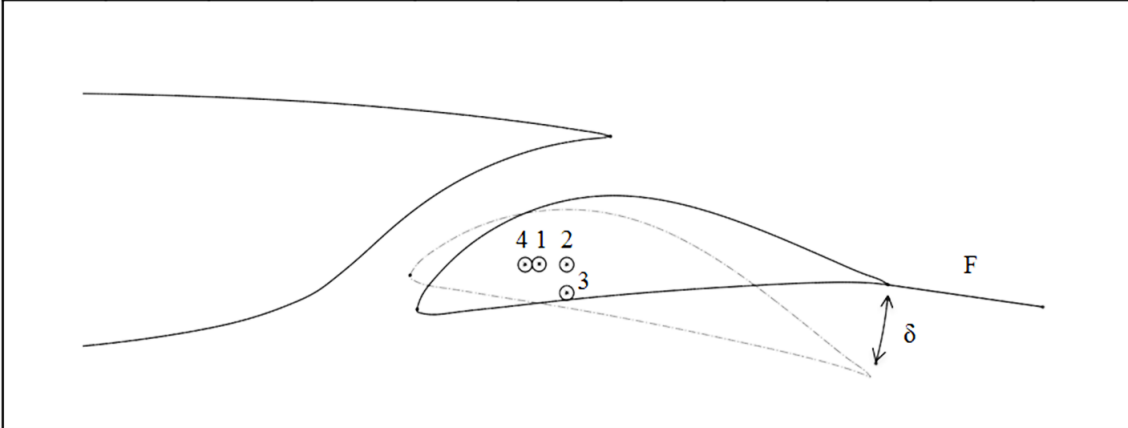


Table 1. Aft-element configurations tested on S414 SNLF airfoil.



Figure 1. S414, slotted, natural-laminar-flow airfoil.

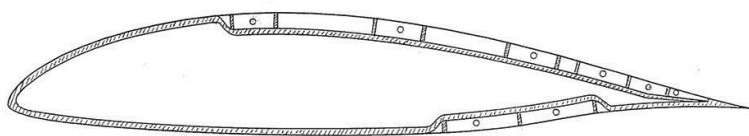


Figure 2. DLR LAMA1 laminar-flow-control (suction) airfoil.



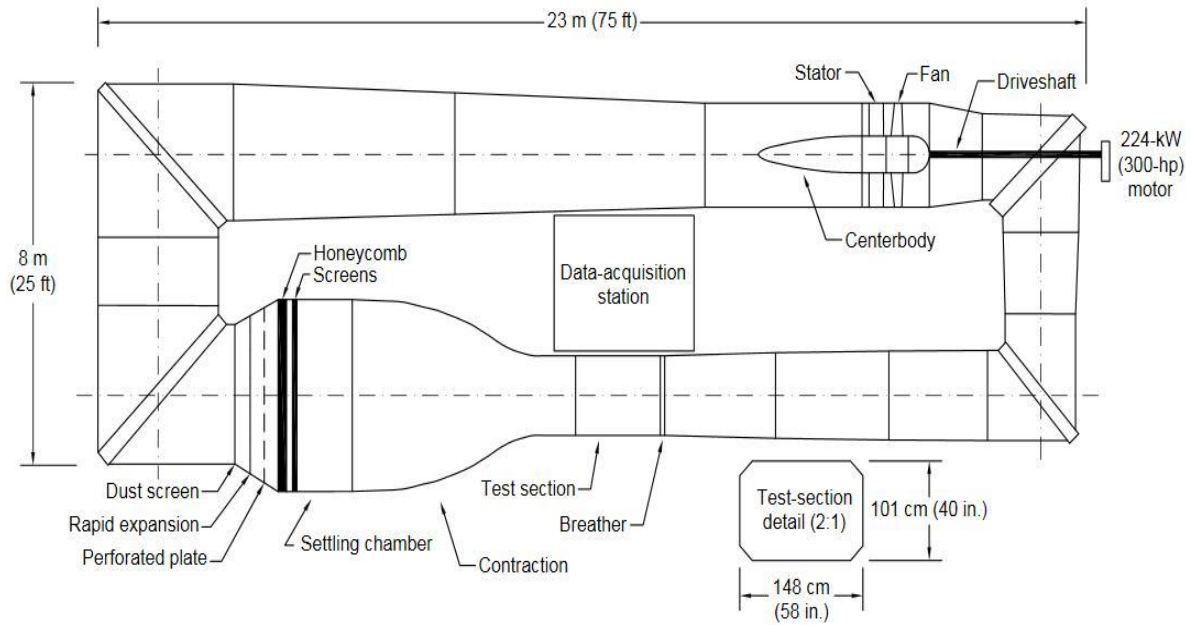


Figure 3. The Pennsylvania State University Low-Speed, Low-Turbulence Wind Tunnel.

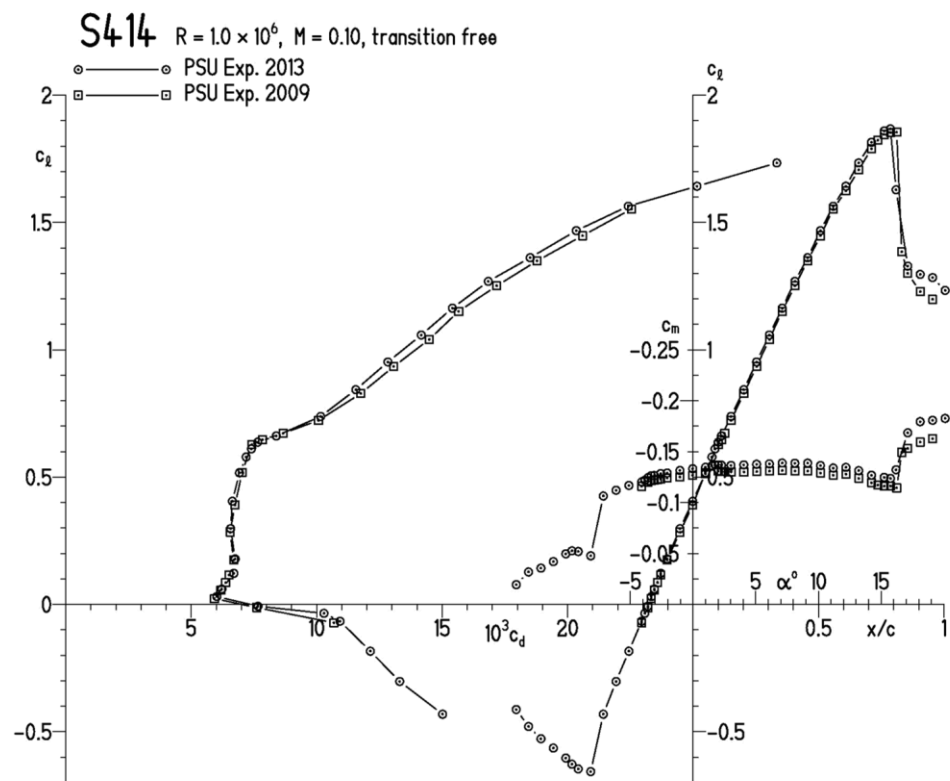


Figure 4. Comparison of current and previous [3] section characteristics of S414 airfoil.

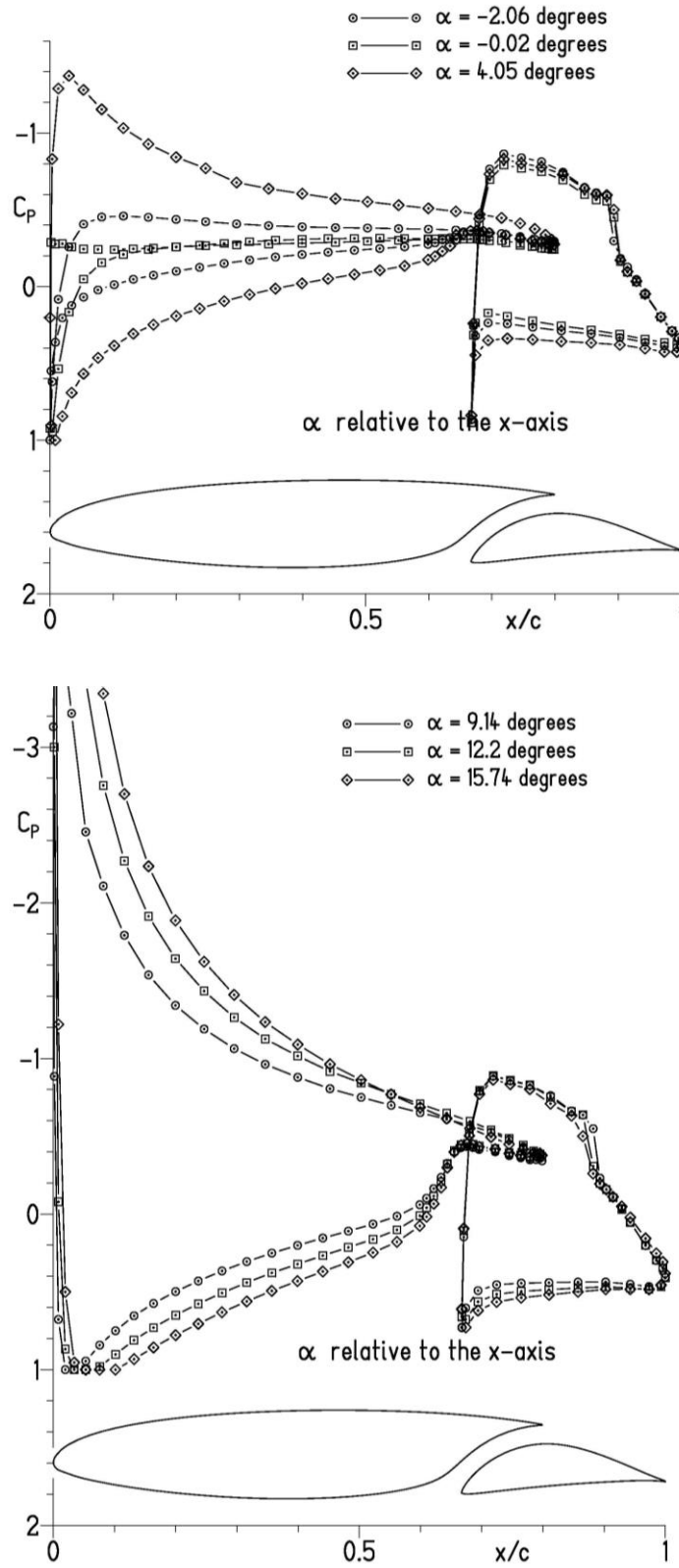


Figure 5. Pressure distributions for baseline configuration for  $R = 1.0 \times 10^6$ .

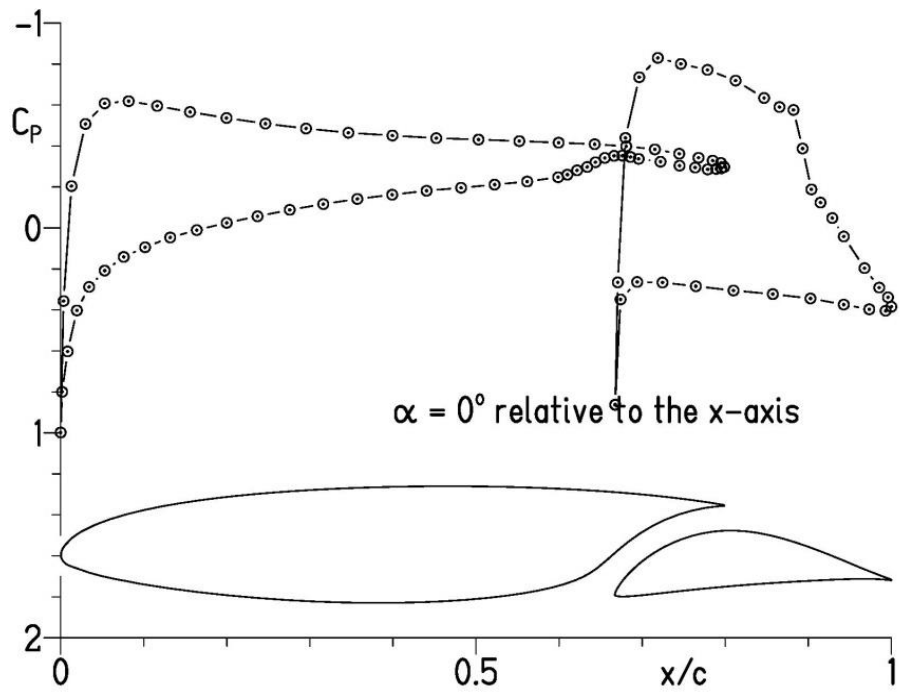


Figure 6. Pressure distribution for baseline configuration (no aft-element rotation or translation) at  $c_l = 0.52$ .

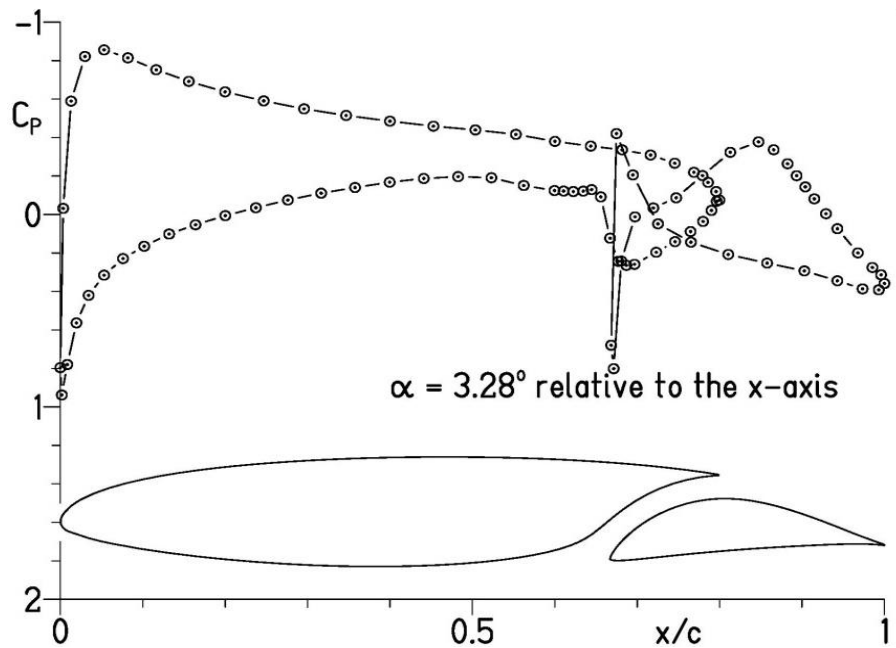


Figure 7. Pressure distribution with aft-element incidence of  $-5$  degrees at  $c_l = 0.49$ .

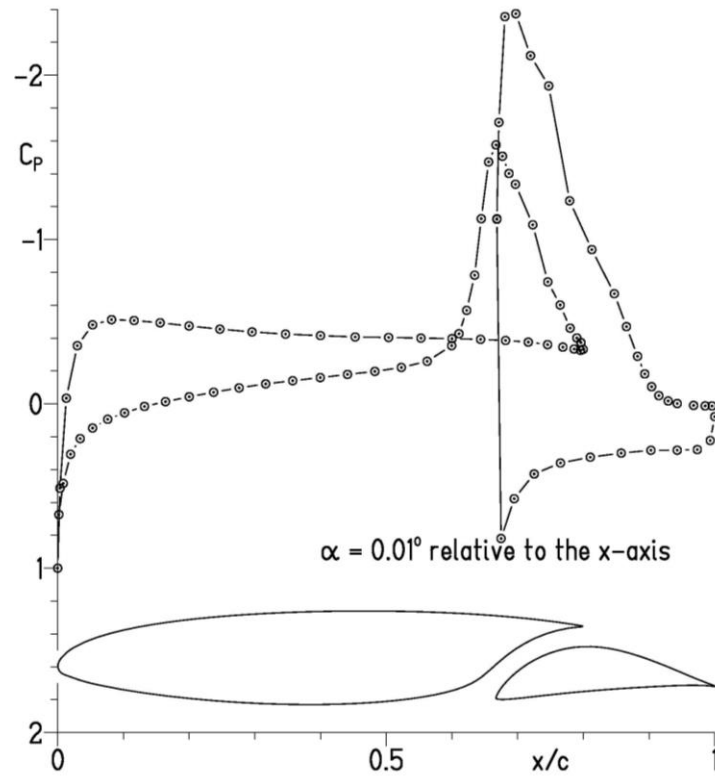


Figure 8. Pressure distribution with aft-element incidence of 5 degree at  $c_l = 0.50$ .

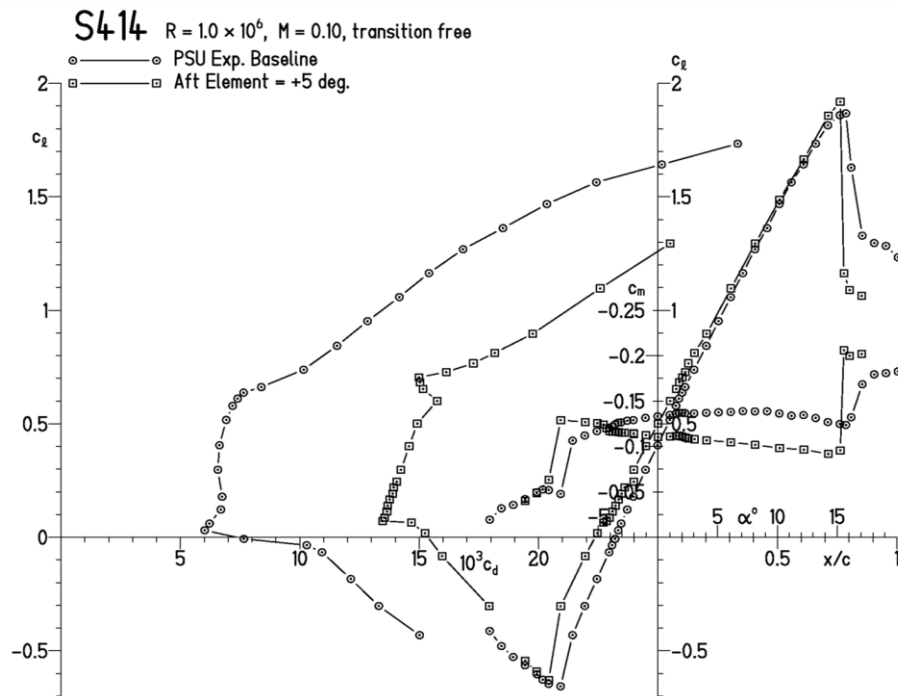


Figure 9. Effect of aft-element incidence on section characteristics of S414 airfoil.

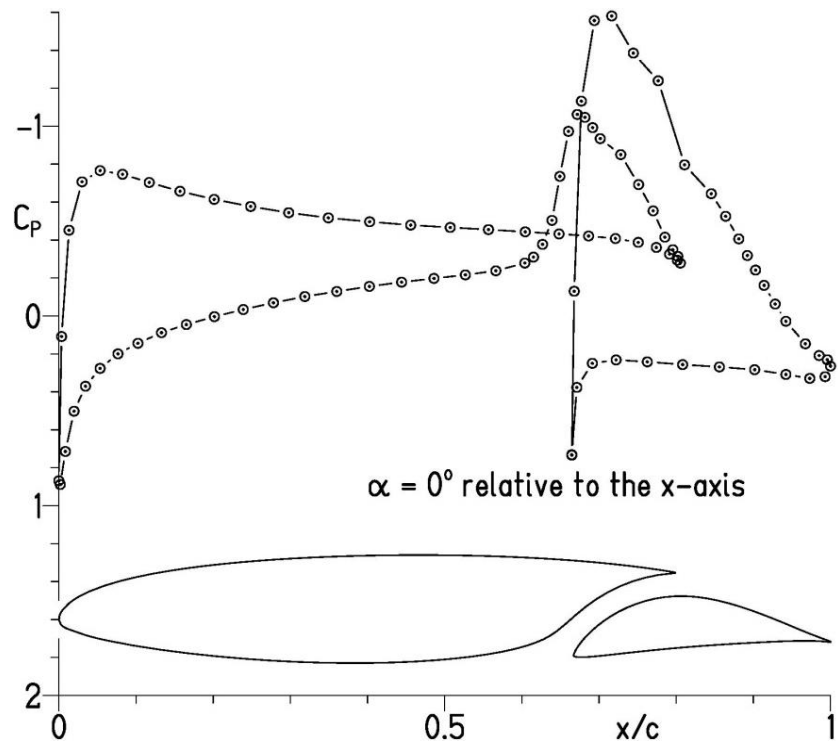


Figure 10. Pressure distribution with aft-element translation of  $\Delta x/c = -0.0083$  and  $\Delta y/c = 0$  at  $c_l = 0.57$ .

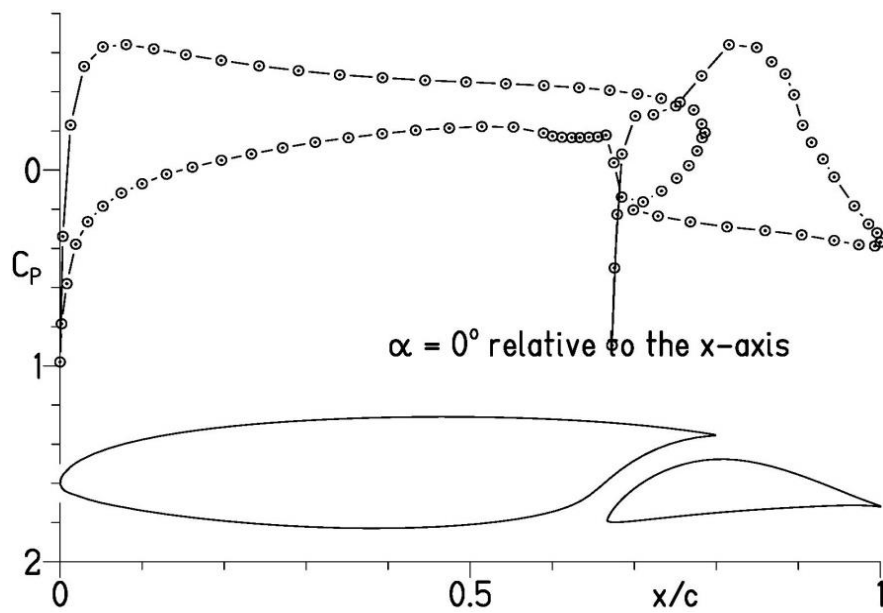


Figure 11. Pressure distribution with aft-element translation of  $\Delta x/c = 0.0167$  and  $\Delta y/c = 0$  at  $c_l = 0.50$ .

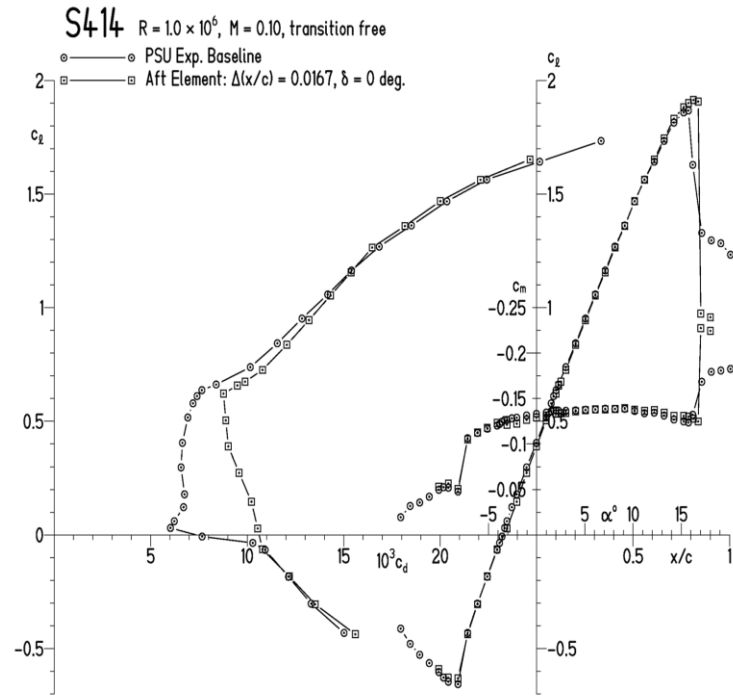


Figure 12. Effect of aft-element translation on section characteristics of S414 airfoil.

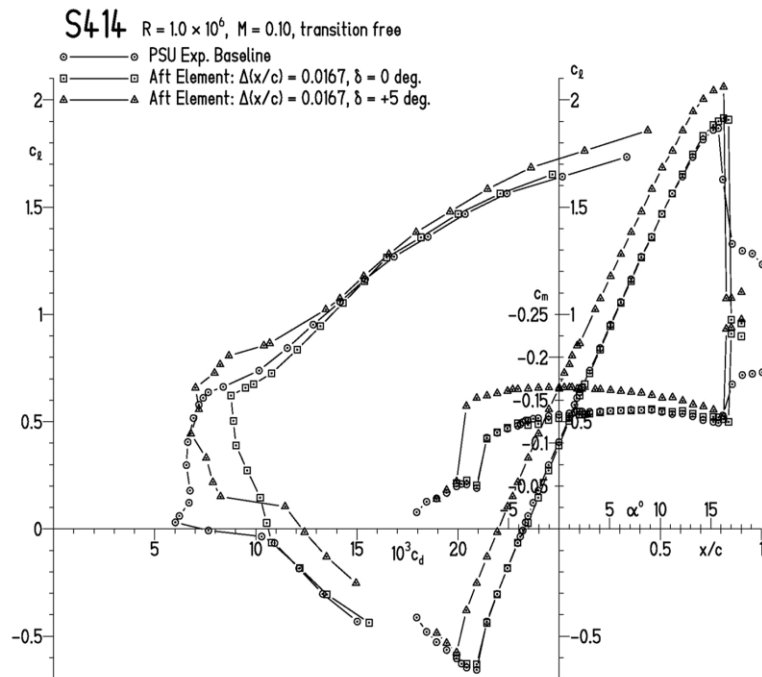


Figure 13. Effect of aft-element rotation plus translation on section characteristics of S414 airfoil.

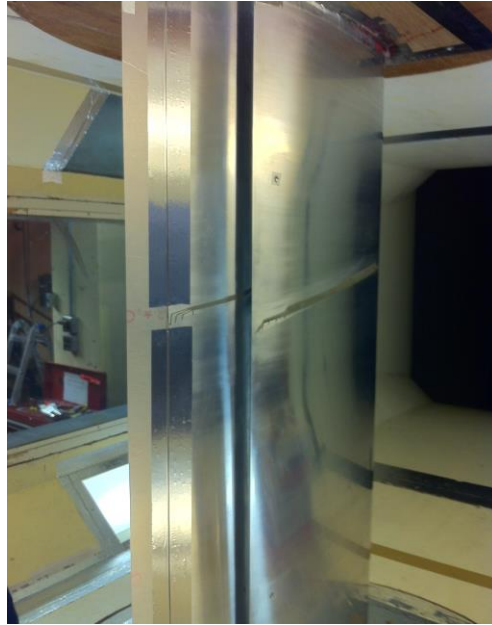


Figure 14. Simulated simple flap attached to aft element of S414 airfoil.

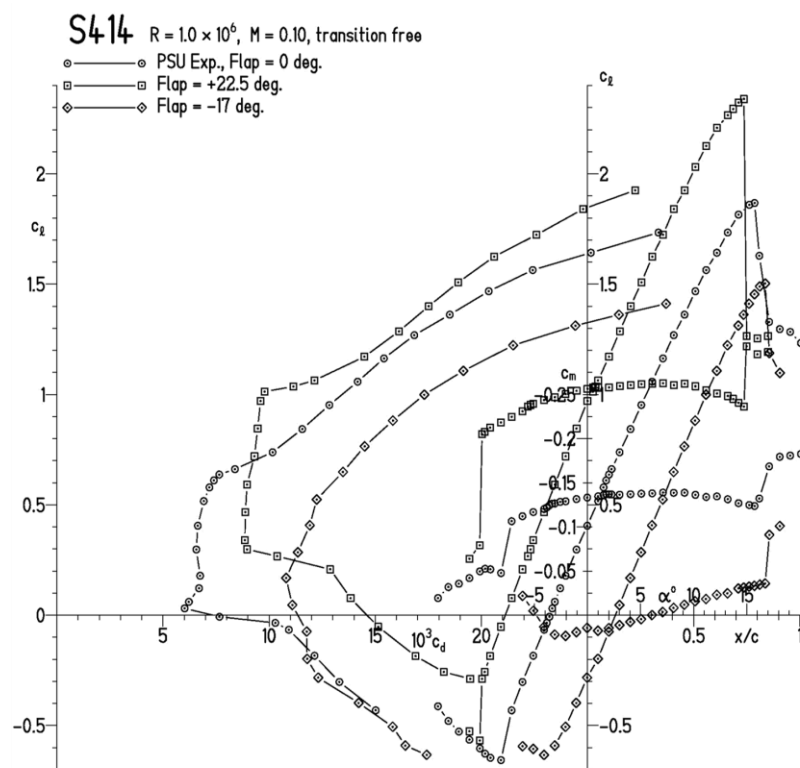


Figure 15. Effect of simulated, aft-element simple flap on section characteristics of S414 airfoil.

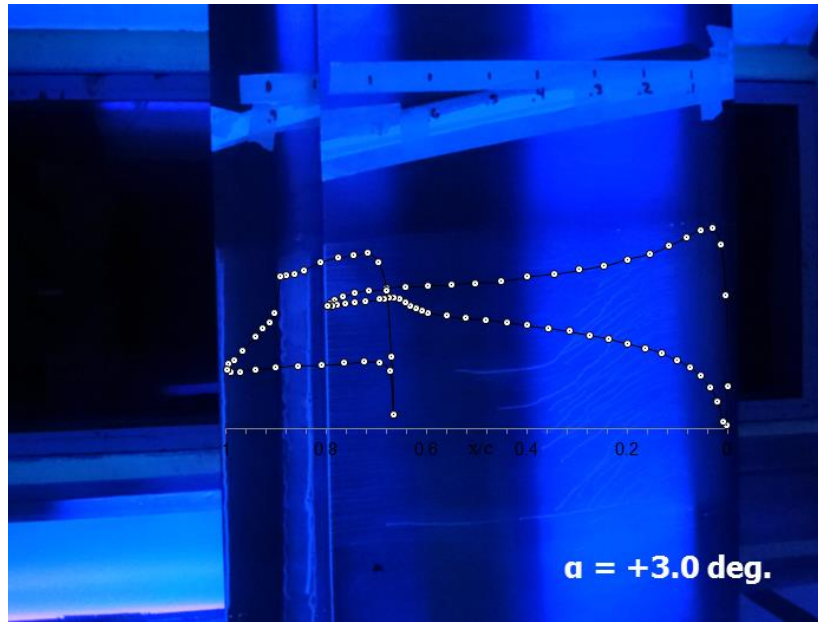


Figure 16. Oil-flow photograph with overlaid pressure distribution at  $\alpha = 3.0^\circ$  (flow from right to left).

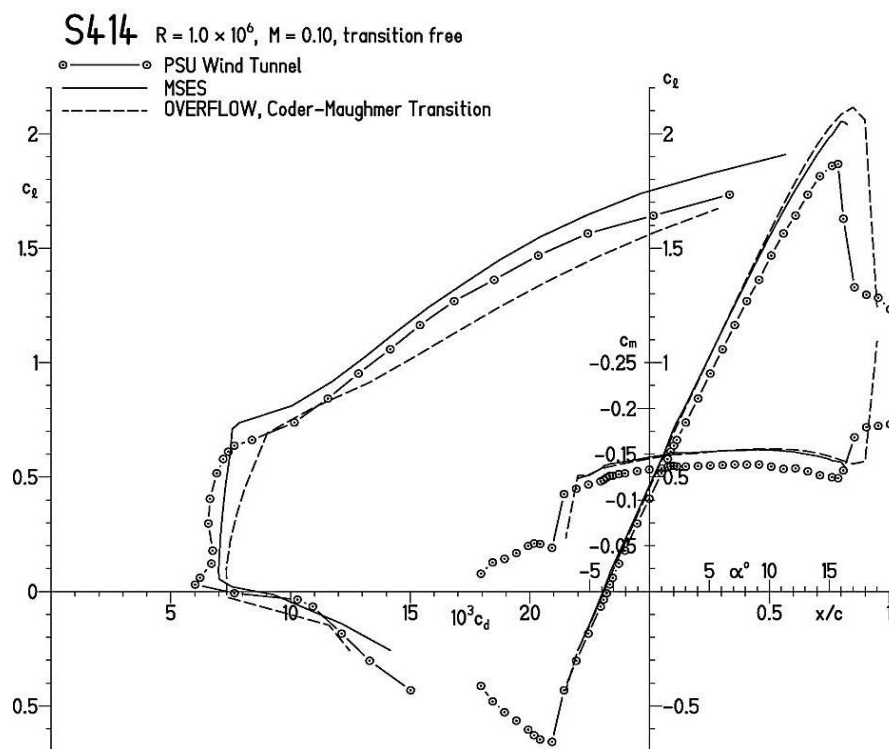


Figure 17. Comparison of theoretical and experimental section characteristics of S414 SNLF airfoil.



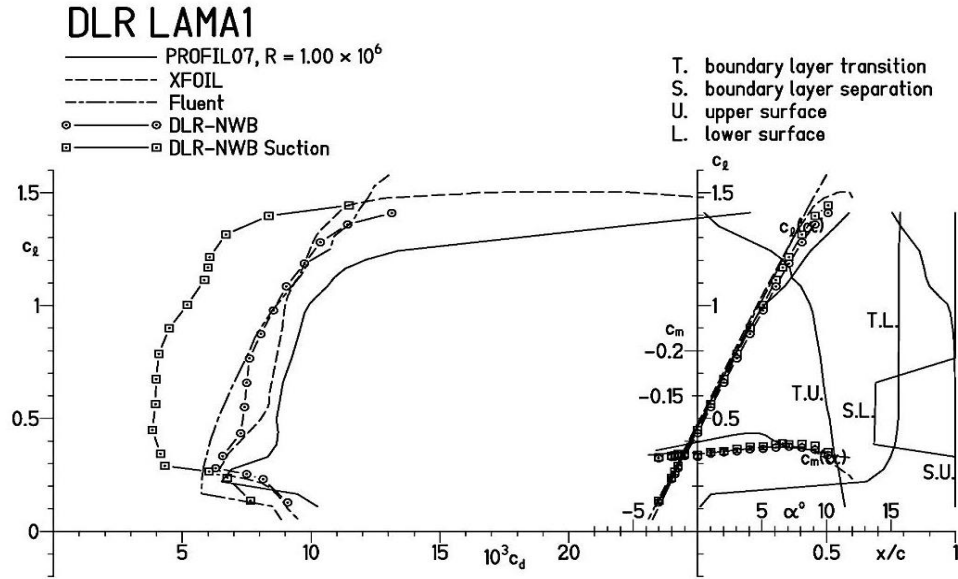


Figure 18. Comparison of theoretical and experimental section characteristics of DLR LAMA1 LFC airfoil.

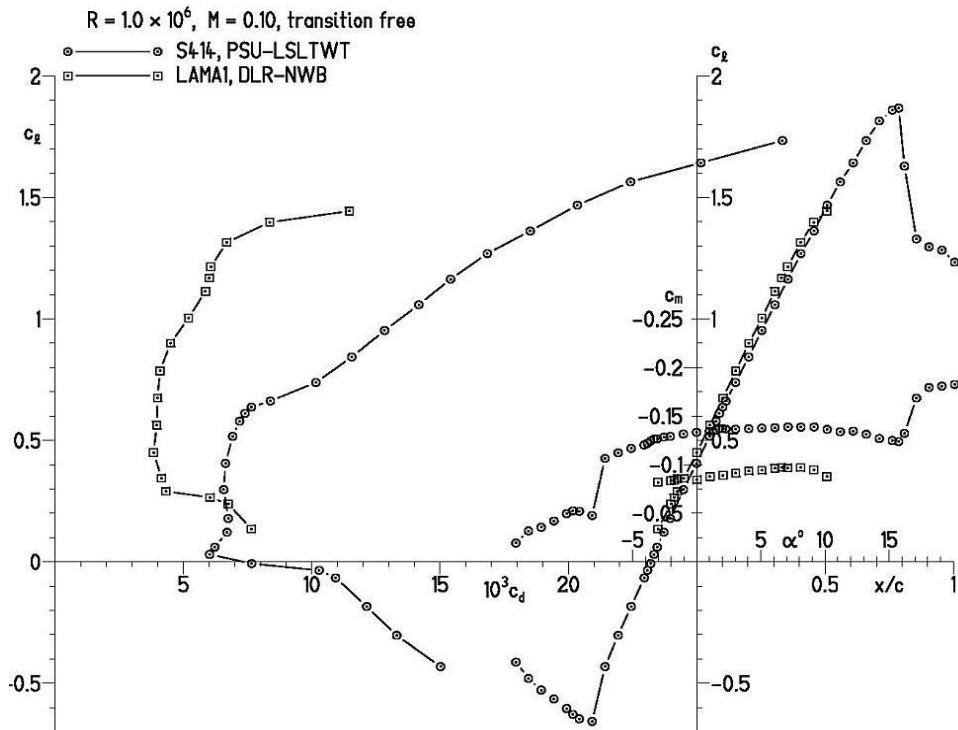


Figure 19. Comparison of experimental section characteristics of S414 SNLF and DLR LAMA1 LFC airfoils.